ARTICLES
PUBLISHED ONLINE: 5 MAY 2013 | DOI: 10.1038/NNANO.2013.71
nature nanotechnology

DNA sequencing using electrical conductance measurements of a DNA polymerase

Yu-Shiun Chen[1,2], Chia-Hui Lee[3], Meng-Yen Hung[3], Hsu-An Pan[2,3], Jin-Chern Chiou[2,4] and G. Steven Huang[2,3]*

The development of personalized medicine—in which medical treatment is customized to an individual on the basis of genetic information—requires techniques that can sequence DNA quickly and cheaply. Single-molecule sequencing technologies, such as nanopores, can potentially be used to sequence long strands of DNA without labels or amplification, but a viable technique has yet to be established. Here, we show that single DNA molecules can be sequenced by monitoring the electrical conductance of a phi29 DNA polymerase as it incorporates unlabelled nucleotides into a template strand of DNA. The conductance of the polymerase is measured by attaching it to a protein transistor that consists of an antibody molecule (immunoglobulin G) bound to two gold nanoparticles, which are in turn connected to source and drain electrodes. The electrical conductance of the DNA polymerase exhibits well-separated plateaux that are ~3 pA in height. Each plateau corresponds to an individual base and is formed at a rate of ~22 nucleotides per second. Additional spikes appear on top of the plateaux and can be used to discriminate between the four different nucleotides. We also show that the sequencing platform works with a variety of DNA polymerases and can sequence difficult templates such as homopolymers.

Accurate DNA sequencing is critical to personalized medicine[1,2] and requires a high-throughput technique that can decode genomes at an affordable price and within a reasonable timeframe[3–6]. In the past decade, next-generation sequencing technologies have been developed that are based on arrayed reactions that sequence amplified DNA targets[7–10]. Compared with first-generation Sanger sequencing, this approach significantly reduces the time required to completely sequence a human genome, but the short read length and high error rate limit its further application to unknown genomes[2,11,12].

Third-generation sequencing (single-molecule sequencing technology) does not require amplification, ligation or cloning, and is expected to provide single-molecule resolution, a long read length and negligible error rate, together with a reduction in cost[11–21]. Such methods typically involve cyclic reactions using fluorescent substrates that are monitored by optical imaging[11,12,14], and have, for example, been used to sequence the M13 viral genome[14].

An alternative third-generation approach is nanopore sequencing, which identifies a molecule by measuring the modulations in the ionic current across a synthetic or biological pore as a DNA molecule is driven through it under an applied potential[16–18]. This approach has been used to read DNA at single-nucleotide resolution by using a phi29 DNA polymerase (Φ29) to control the rate of DNA translocation through a MspA nanopore[17]. Oxford Nanopore Technologies has also reportedly used a prototype nanopore device to decode a viral genome in a single pass of a complete DNA strand[19,20].

However, the performance of commercialized third-generation technology is currently only comparable to next-generation sequencing methods[13,22] and the problems of short read lengths and high error rates have yet to be solved[23,24]. Accordingly, a third-generation sequencing method that can provide high-quality sequencing data with long read lengths and low error rates is still required.

DNA polymerase is an enzyme that catalyses the synthesis of DNA when provided with the four deoxynucleoside-5′-triphosphates (dATP, dTTP, dCTP, dGTP; abbreviated dNTP), a template strand and a primer with a free 3′-OH end[25]. During the reaction, a complementary dNTP is chosen based on template base-pairing, which forms a phosphodiester bond to the 3′-OH of the primer and releases pyrophosphate. The chain elongates as DNA polymerase proceeds along the template strand, before dissociating from the template. The interaction between a dNTP and DNA polymerase exhibits a classical Michaelis–Menten mechanism consisting of substrate-binding (base-pairing) and bond-formation steps[26].

Electrical conductivity is a useful tool for monitoring single-molecule dynamics[27]. The sensitivity, reproducibility, reversibility, convenience and dynamic response of conductance measurements should also be beneficial in monitoring enzyme dynamics. Therefore, by tracking the electrical conductance of DNA polymerase during replication, it should be possible to identify sequence-specific nucleotide incorporation due to differences in base pairing and chemical composition. In particular, the electrostatic reorganization and non-covalent interactions between the enzyme and the substrate may enhance the electron transfer environment[28], and the enzyme–substrate complex could become more conductive during catalysis, particularly during the reorientation and redistribution of charges in the transition state.

In this work, we aim to develop a single-molecule sequencing technology based on the measurement of the electrical conductance of DNA polymerase as nucleotides are incorporated into the growing DNA strand. A protein transistor, which provides stable conductance readings, was designed to hold a DNA polymerase

[1]Department of Biological Science and Technology, National Chiao Tung University, 1001 University Road, Hsinchu, Taiwan, ROC, [2]Biomedical Electronics Translational Research Center, National Chiao Tung University, 1001 University Road, Hsinchu, Taiwan, ROC, [3]Department of Materials Science and Engineering, National Chiao Tung University, 1001 University Road, Hsinchu, Taiwan, ROC, [4]Institute of Electrical and Control Engineering, National Chiao Tung University, 1001 University Road, Hsinchu, Taiwan, ROC. *e-mail: gstevehuang@mail.nctu.edu.tw

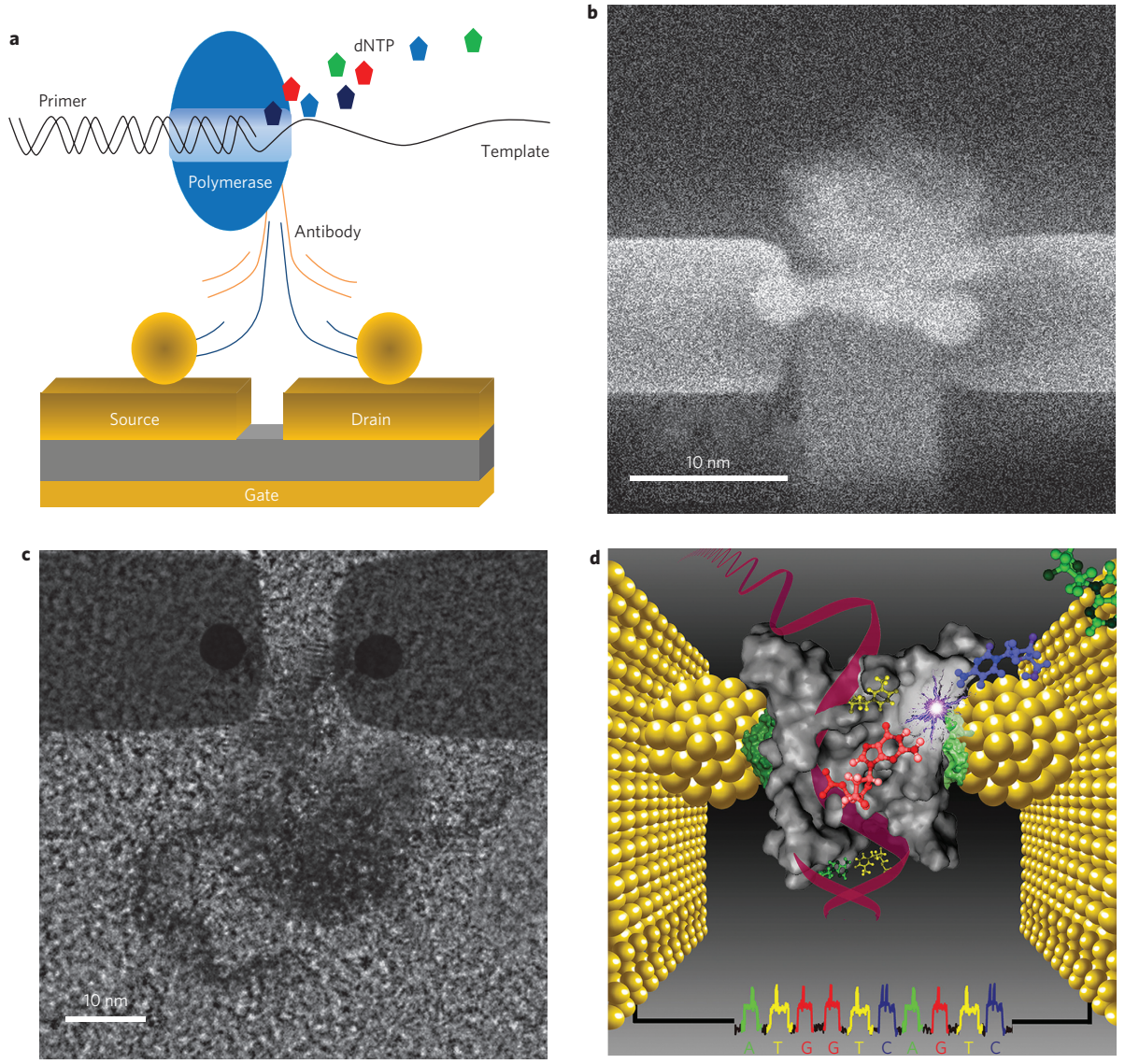

Figure 1 | The protein transistor–DNA polymerase sequencing platform. a, Schematic representation of the single-molecule sequencing platform. The Φ29 (light blue) is conjugated to a secondary antibody (beige lines) and binds the Fc domain of IgG (blue lines). The primer-annealed oligonucleotide template is assembled on the Φ29. Substrates are shown as pentagons. **b**, Scanning electron microscopy (SEM) image of the Φ29-conjugated proT. **c**, Transmission electron microscopy (TEM) image of Φ29-conjugated proT with bound template. Oligo 3 is annealed with primer and bound onto the immobilized Φ29. The sequencing reaction is initiated by a short pulse of dNTPs. The polymerase complex with partially sequenced template is stained and imaged by TEM. **d**, Schematic drawing of the single-molecule sequencing platform projecting from the Φ29 polymerase. The electrical conductance of Φ29 (grey) is measured using gold nanoparticles attached to the source and drain electrodes. Φ29 sits between two electrodes while incorporating nucleotides onto the growing strand of DNA (pink). The incorporation of incoming nucleotides base pairing with the template is shown at the white area of the polymerase. The colour-decoded conductance trajectory is shown under the Φ29. Sequence of Oligo 3: 5′-aagaagttac gattgcgcgg gtcctcagaa tgaacattca gagaatcata ctaacaccag aaaccagtac ataggccaca gcgttcttca acgccggtac gaattactcc ccattgaaga cgccgcggagccaag-3′.

during the synthesis of a new strand[29]. The protein transistor consists of an immunoglobulin G (IgG) bearing two gold nanoparticles, which are separately attached to two electrodes, and specific antibody binding ensures the self-assembly of the IgG into the integrated circuit. The electrical conductivity of the DNA polymerase can then be directly measured by conjugating the polymerase to the protein transistor.

The protein transistor–DNA polymerase device

The sequencing platform is shown schematically in Fig. 1. Electron-beam lithography was used to create 10 nm gaps between 50-nm-wide electrodes. Nanoparticles (diameter, 5 nm) were brought onto the edge of the electrode pairs with the tip of an atomic force microscope. The nanoparticle-charged device was covered with polydimethylsiloxane using a pre-moulded liquid channel (100 nm wide and 20 nm deep) to protect the device from physical damage. The IgG was delivered by passing 1 pg ml^{-1} of anti-nanoparticle IgG through the liquid channel at a flow rate of 0.1 μl s^{-1} (ref. 30). The protein transistor was successfully assembled when a stable source–drain current (I_{SD}) was detected.

The Φ29 is a replicative polymerase with long processivity and low error rate[31]. It was crosslinked to a secondary antibody that recognizes the Fc domain of the protein transistor. The column-purified Φ29 conjugate was then brought to the protein transistor and bound to the IgG component of the transistor. The binding of the Φ29 conjugate caused an irreversible increase in I_{SD} of

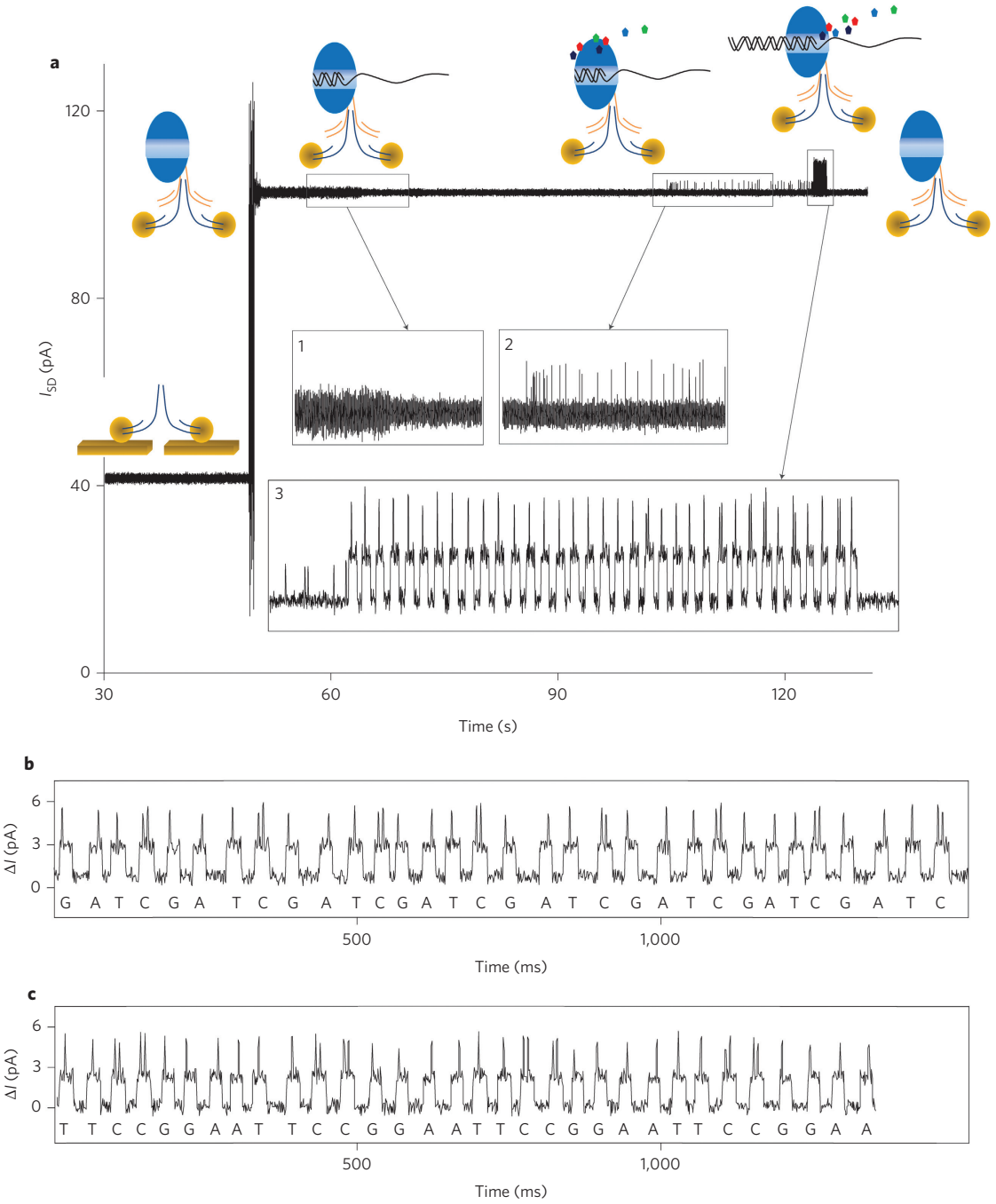

Figure 2 | Monitoring the assembly of the protein transistor–Φ29 platform and identifying the different bases with electrical conductance measurements. **a**, Step-by-step assembly of protein transistor–Φ29, as monitored by electrical conductance. The proposed status of the sequencing complex is drawn as a cartoon and indicates the relative positions of the trajectory. The conductance of the protein transistor was initially 43 pA. The Φ29–IgG conjugate binds to the Fc domain of proT and causes a sudden fluctuation in conductance, which finally settles at 102 pA with the noise level at 5 pA. The template–primer annealing complex binds at the active site of Φ29 and stabilizes the conductance. The noise level is reduced to 1 pA (inset 1), and the addition of dNTPs triggers the enzymatic reaction. Reversible binding between the substrate and polymerase appears at the early stage of the reaction trajectory, forming stochastic spikes (inset 2). This is followed by consecutive sequencing plateaux that are 3 pA in height (inset 3). The trajectory returns to a non-active level after the synthesized double-stranded DNA falls off the polymerase. **b**, Conductance trajectory of a protein transistor–Φ29 sequencing template carrying GATC repeats. The nucleotide sequence is labelled under each plateau. **c**, Conductance trajectory of the protein transistor–Φ29 sequencing template carrying TTCCGGAA repeats.

~60 pA when the source–drain (V_{SD}) and gate (V_G) voltages were set to 9.0 V and 3.0 V, respectively (Fig. 2).

Electron micrographs of the transistor–Φ29 construct revealed a spatial arrangement where Φ29 connects to the secondary antibody, which binds to the Fc domain of the first antibody, and then the first antibody binds nanoparticles on the source and drain electrodes (Fig. 1b). The stepwise assembly of the transistor–Φ29 was monitored by electrical conductivity (Fig. 2). It should be noted that to obtain a pico-ampere signal, all measurements were performed in a shielding room to minimize electromagnetic and radiofrequency

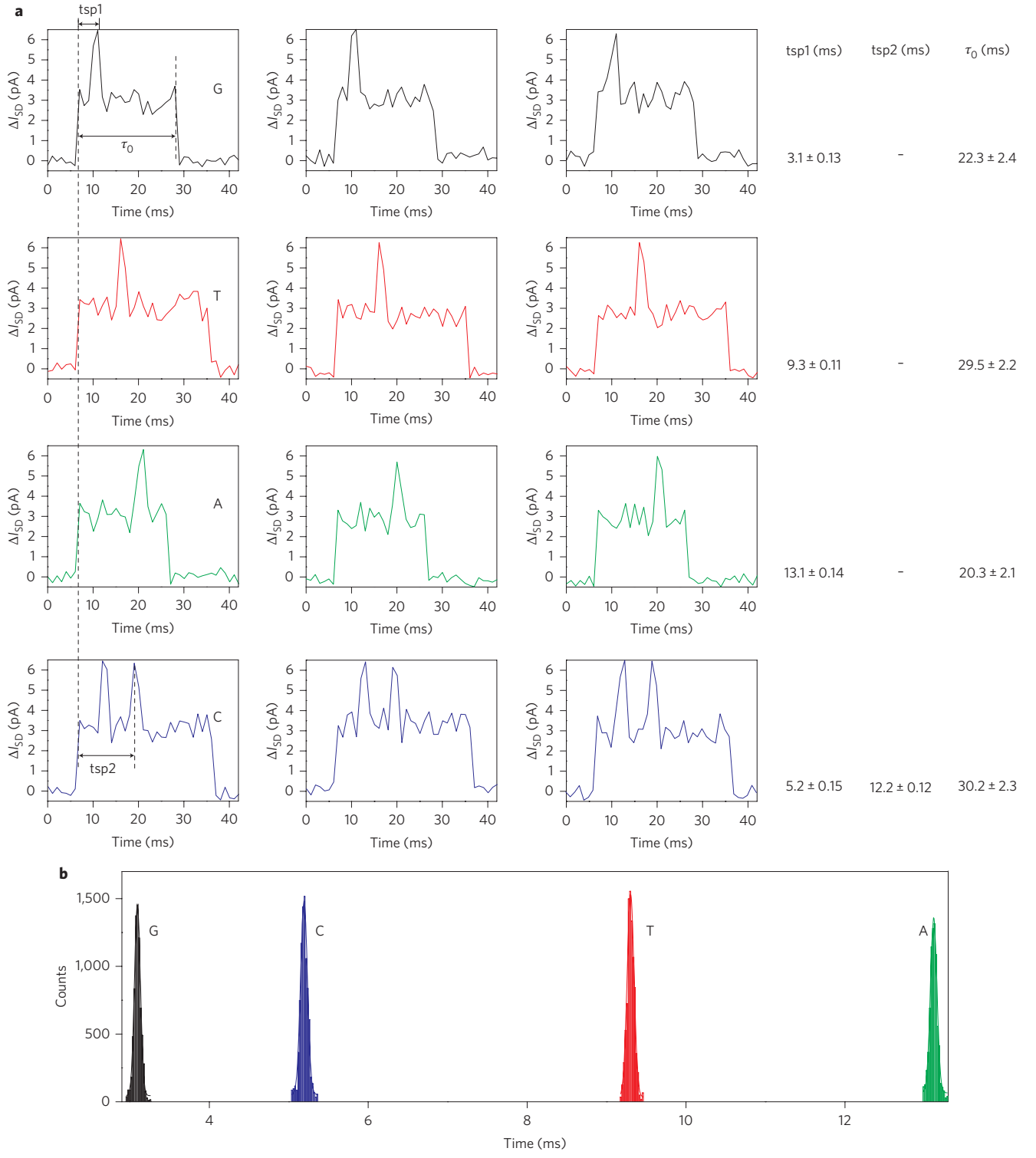

Figure 3 | Base-calling criteria for G, T, A and C nucleotides. a, The timing of spikes after the rise of the plateaux (tsp1 and tsp2) enables base-calling. Plateau width (τ_0) is used to distinguish pyrimidines and purines. Three sets of plateaux representing G, T, A, and C are randomly selected from raw data. Mean ± standard deviation is shown on the right. The results are calculated from more than 50,000 plateaux. **b**, The sharp distribution of tsp1, indicating the robustness of the method.

interference. To reduce signal decay, superconducting materials were used for the interface between transistor and probes.

The dynamic response of an electrical signal transmitted through a conjugated protein may limit the performance of the sequencing platform. The dynamic response was therefore measured by sending a high-frequency laser pulse to a quantum dot-conjugated protein transistor and measuring the photon-induced fluctuation in the electrical signal (Supplementary Fig. S1). The laser waveform at a frequency of $1.7 \times 10^9\ s^{-1}$ was detected by means of electrical conductance with fidelity, indicating that the system was capable of providing a subnanosecond dynamic response. The turnover rate of Φ29 ranges from 20 to 150 nt s^{-1}, and the sequencing

Table 1 | Heights and widths of the plateaux sequenced by various polymerases.

	Hr* (pA)				τ_0 (ms)			
	G	T	A	C	G	T	A	C
Φ29†	3.1±0.41	3.01±0.41	3.0±0.43	3.1±0.42	22.3±2.4	29.5±2.2	20.3±2.1	30.2±2.3
T4	3.2±0.42	3.2±0.58	3.1±0.43	3.3±0.54	22.2±2.5	29.2±2.4	20.1±2.3	30.5±2.3
T7	3.3±0.42	3.6±0.43	3.1±0.4	3.7±0.41	23.1±2.3	26.4±2.3	19.2±2.1	28.3±2.2
Pol I	3.4±0.8	3.7±0.68	3.2±0.72	3.8±0.67	20.1±2.4	25.4±2.4	26.2±2.3	33.2±2.6

*Hr, height of the plateaux. τ_0, width of the plateaux.
†Symbols: Φ29, phi29 DNA polymerase; T4, T4 DNA polymerase; T7, T7 DNA polymerase; Pol I, *E. coli* DNA polymerase I.

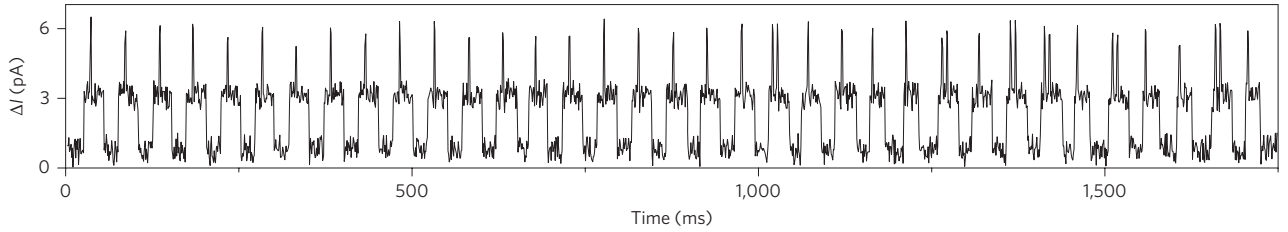

Figure 4 | Conductance trajectory of the protein transistor platform sequencing a difficult template. Template carrying homopolymer is sequenced by Φ29. The decoded sequence (5′ to 3′) is $(t)_{20}$cttggctccgcggcg.

reaction occurs within a millisecond timescale. Thus, the time bin was set to 1 μs during the measurement.

Identifying bases with electrical conductance

The sequential incorporation of nucleotides, as well as the identity of the four different nucleotides, can be detected by their characteristic conductance responses. A synthetic template carrying GATC repeats—Oligo 1 (Supplementary Table S1)—was annealed with a complementary primer and loaded onto the immobilized Φ29. The fluctuation of noise eventually stabilized if sufficient time was allowed (Fig. 2a). However, the binding of the annealed template helped to stabilize the fluctuating conductance of the replicating complex, as shown by the reduction of noise levels in the I_{SD} versus time plot (Fig. 2a, inset 1).

Synthesis of the complementary DNA strand was triggered by passing 1 μM dNTPs through the sequencing platform. The conductance trajectory was then recorded during polymerization (Fig. 2a). Spikes with a height of ∼3 pA appeared stochastically after the injection of dNTPs (Fig. 2a, inset 2). These spikes were probably caused by the rapid binding and disassociation of the polymerase and nucleotides. The disordered response was followed by grouped but well-separated plateaux that were ∼3–4 pA in height (Fig. 2a, inset 3). The shape of the plateaux could be used to identify the stages of sustained enzyme–substrate binding, catalysis and pyrophosphate release. The appearance of sequential plateaux indicated stepwise base pairing and nucleotide incorporation into the growing strand. The rate of plateau formation was ∼22 nt s^{-1}, which matches the turnover rate of Φ29 at 25 °C (refs 32–35). DNA replication continued to fill in the complementary sequence until falloff of the template.

The binding of a nucleotide to the active site of Φ29 promoted conductance. The binding between the nucleotide and the polymerase was followed by bond formation, the release of pyrophosphate, sliding down of the double-stranded DNA, and active site evacuation, which created room for the next nucleotide. One complete reaction cycle appeared as a plateau in the conductance trajectory.

The four different nucleotides were distinguished by their characteristic spike patterns. dG, dT and dA exhibited a single spike of 3 pA above the plateau at the front, middle and end of the plateau, respectively, while dC exhibited multiple spikes. With a sudden increase or decrease in conductance, spikes indicate a temporary change in electrostatic organization (Fig. 2b). The times of the spikes after the rise of the plateau (tsp1) are 3.1±0.13 ms for G, 9.3±0.11 ms for T and 13.1±0.14 ms for A. Two spikes, at 5.2±0.15 ms (tsp1) and 12.2±0.12 ms (tsp2), always occur for C (Fig. 3). The spike patterns seem irrelevant to the number of hydrogen bonds or to the chemical composition of the nucleosides. The widths of the plateaux are 22.3±2.4, 29.5±2.2, 20.3±2.1 and 30.2±2.3 ms for dG, dT, dA and dC, respectively. A focused width distribution indicates that the catalytic activity of the polymerase is constant and non-stochastic.

We also noticed that the plateau width for pyrimidines (T and C) was longer than for purines (G and A), and this correlation between plateau shape and nucleotide sequence was verified by performing a sequencing reaction with a template carrying GGAATTCC repeats (Fig. 2c, Supplementary Table S1). Base-calling was verified by giving one type of nucleotide at a time. The characteristic electrical signature appeared only when the corresponding nucleotide was provided (Supplementary Fig. S2). Furthermore, if the polymerization was terminated by dideoxynucleotide, the addition of dNTP gave only binding spikes, without reaction plateaux (Supplementary Fig. S3). Sequencing on randomly mixed templates also indicated the accuracy of base-calling (Supplementary Fig. S4). From shape analysis, consistent recognition was established starting from the beginning of the plateaux and extending over ∼90% of the plateaux. Variations in width and shape frequently occurred at the end of the plateaux—after the last spike in the cases of dA and dC. This result demonstrates that single-molecule sequencing could be achieved by monitoring the electrical conductance of a polymerase during the synthesis of a growing DNA strand. The base-calling criteria are summarized in Fig. 3.

Comparing different DNA polymerases

The association between nucleotides and their corresponding plateau shape was further explored by examining the patterns seen with other DNA polymerases. Reaction trajectories were obtained for T4 DNA polymerase (T4), T7 DNA polymerase (T7) and DNA polymerase I (Pol I) sequencing on Oligo 3 (Supplementary Fig. S5). The plateau widths and heights from Φ29, T4, T7 and Pol I shared a high degree of similarity, with only minor variations (Table 1). Pol I exhibited a broader distribution of plateau height than Φ29, T4 and T7, which exhibited more focused distributions

of both height and width. The shape of the plateaux corresponding to nucleotides G, T, A and C remained distinguishable. The association between plateaux and nucleotides for various polymerases indicates that the molecular mechanisms of base pairing and bond formation are common features shared by DNA polymerases. Under conditions where the plateau shapes were sufficient to sequence a DNA molecule, the inherently long processivity and low error rate of the Φ29, T4 and T7 polymerases made them good candidates for genomic sequencing.

Templates containing a stretch of a single nucleotide are known to be difficult for sequencing, and such templates frequently give read errors in many sequencing technologies[14,18]. To explore the utility of our new sequencing platform, a template containing 20 consecutive T nucleotides was sequenced using Φ29 (Fig. 4). The results indicate that the protein transistor platform is indeed capable of resolving 20 T nucleotides without ambiguous reading.

The measured conductance trajectories were consistent with previous studies examining the kinetics of DNA polymerases and single-molecular enzymes. The Michaelis–Menten mechanism proposes a reversible binding step that occurs before the formation of an enzyme–substrate complex, which is followed by catalysis and product release. This mechanism is corroborated by the observed binding spikes and groups of reaction plateaux (Fig. 2a, insets 2 and 3). Spikes are a result of rapid increases and decreases in conductance corresponding to reversible substrate binding. Once a stable enzyme–substrate complex is formed, catalytic events proceed that can be described by examining the plateaux. The onset of each reaction is stochastic, and this is consistent with observations made using single-molecule fluorescence[36]. However, the sharp distribution of plateau widths indicates that catalysis obeys precisely designed molecular steps. This evidence for constant catalysis has not been reported previously, further highlighting the molecular resolution of the current platform.

A few questions remain regarding the read length, error rate and high throughput ability of this platform before it can be applied in a clinical setting[11]. Φ29, T4 and T7 are replicative polymerases with exceptional strand displacement and processive synthesis properties that have the ability to work on difficult templates containing complex secondary structures. However, the single-molecule catalytic mechanism needs to be explored to identify a candidate polymerase appropriate for genomic sequencing. Oligo 3 was sequenced more than 20 times by all four polymerases. We were unable to find an error in more than 50,000 nucleotides of our sequencing data, which demonstrates the extraordinary accuracy of this system. The self-assembly of protein transistors permits the construction of multiple sequencing devices on the same chip, although the difficulty of acquiring high-speed parallel electrical signals with sub-pico-ampere noise levels remains[29].

Conclusions

We have developed a sequencing strategy based on electrical conductance measurements of a DNA polymerase conjugated to a protein transistor. This sequencing strategy works with different polymerases and efficiently processes difficult templates containing long stretches of T nucleotides.

Single-molecule electrical conductance is a versatile platform that can be readily adapted to most enzymatic systems by secondary antibody conjugation or by direct crosslinking. As a result, the approach can be used to study a range of enzymes that cannot be conveniently labelled for a fluorescence resonance energy transfer approach, such as enzymes composed of multiple subunits. The self-assembly of the protein transistor also suggest that an integrated and parallel assaying system could be developed. However, it should be noted that the current platform might be limited by the size of the conjugated enzyme–product complex. For polymerizing reactions such as the synthesis of the second strand of DNA, the growing mass of enzyme–product might physically retard the ongoing polymerization reaction or gradually change the conductance, causing unnecessary noise in the current reading. Another limitation is the possible alteration in activity by immobilization of the enzyme molecule. Although the catalytic activity of Φ29 immobilized on the protein transistor is comparable to ensemble studies, much work is required to correlate the single-molecule trajectory obtained by this platform to molecular mechanism of DNA replication. Finally, the complex composition of biological fluid could create significant noise. This could limit the application of this device in *in vivo* single-cell measurements.

Received 24 September 2012; accepted 25 March 2013; published online 5 May 2013; corrected after print 11 July 2013 and 28 August 2013

References

1. Schatz, M. C., Delcher, A. L. & Salzberg, S. L. Assembly of large genomes using second-generation sequencing. *Genome Res.* **20,** 1165–1173 (2010).
2. Shendure, J. & Ji, H. Next-generation DNA sequencing. *Nature Biotechnol.* **26,** 1135–1145 (2008).
3. Hunkapiller, T., Kaiser, R. J., Koop, B. F. & Hood, L. Large-scale and automated DNA sequence determination. *Science* **254,** 59–67 (1991).
4. Sanger, F. *et al.* Nucleotide sequence of bacteriophage ΦX174 DNA. *Nature* **265,** 687–695 (1977).
5. Shendure, J., Mitra, R. D., Varma, C. & Church, G. M. Advanced sequencing technologies: methods and goals. *Nature Rev. Genet.* **5,** 335–344 (2004).
6. Sherwood, P. DNA from Alberts to Zinder. *Nature* **422,** 806–807 (2003).
7. Ronaghi, M., Karamohamed, S., Pettersson, B., Uhlen, M. & Nyren, P. Real-time DNA sequencing using detection of pyrophosphate release. *Anal. Biochem.* **242,** 84–89 (1996).
8. Bentley, D. R. Whole-genome re-sequencing. *Curr. Opin. Genet. Dev.* **16,** 545–552 (2006).
9. Turcatti, G., Romieu, A., Fedurco, M. & Tairi, A. P. A new class of cleavable fluorescent nucleotides: synthesis and optimization as reversible terminators for DNA sequencing by synthesis. *Nucleic Acids Res.* **36,** e25 (2008).
10. Shendure, J. *et al.* Accurate multiplex polony sequencing of an evolved bacterial genome. *Science* **309,** 1728–1732 (2005).
11. Kircher, M. & Kelso, J. High-throughput DNA sequencing—concepts and limitations. *Bioessays* **32,** 524–536 (2010).
12. Schadt, E. E., Turner, S. & Kasarskis, A. A window into third-generation sequencing. *Hum. Mol. Genet.* **19,** R227–R240 (2010).
13. Li, Y. & Wang, J. Faster human genome sequencing. *Nature Biotechnol.* **27,** 820–821 (2009).
14. Harris, T. D. *et al.* Single-molecule DNA sequencing of a viral genome. *Science* **320,** 106–109 (2008).
15. Levene, M. J. *et al.* Zero-mode waveguides for single-molecule analysis at high concentrations. *Science* **299,** 682–686 (2003).
16. Cherf, G. M. *et al.* Automated forward and reverse ratcheting of DNA in a nanopore at 5-Å precision. *Nature Biotechnol.* **30,** 344–348 (2012).
17. Manrao, E. A. *et al.* Reading DNA at single-nucleotide resolution with a mutant MspA nanopore and Φ29 DNA polymerase. *Nature Biotechnol.* **30,** 349–353 (2012).
18. Schneider, G. F. & Dekker, C. DNA sequencing with nanopores. *Nature Biotechnol.* **30,** 326–328 (2012).
19. Elizabeth, P. Search for pore-fection. *Science* **336,** 534–537 (2012).
20. Michael, E. Oxford Nanopore announcement sets sequencing sector abuzz. *Nature Biotechnol.* **30,** 295–296 (2012).
21. Gupta, P. K. Single-molecule DNA sequencing technologies for future genomics research. *Trends Biotechnol.* **26,** 602–611 (2008).
22. Pushkarev, D., Neff, N. F. & Quake, S. R. Single-molecule sequencing of an individual human genome. *Nature Biotechnol.* **27,** 847–850 (2009).
23. Bashir, A. *et al.* A hybrid approach for the automated finishing of bacterial genomes. *Nature Biotechnol.* **30,** 701–707 (2012).
24. Koren, S. *et al.* Hybrid error correction and *de novo* assembly of single-molecule sequencing reads. *Nature Biotechnol.* **30,** 692–700 (2012).
25. Lehman, I. R., Bessman, M. J., Simms, E. S. & Kornberg, A. Enzymatic synthesis of deoxyribonucleic acid. I. Preparation of substrates and partial purification of an enzyme from *Escherichia coli*. *J. Biol. Chem.* **233,** 163–170 (1958).
26. Sanger, F., Nicklen, S. & Coulson, A. R. DNA sequencing with chain-terminating inhibitors. *Proc. Natl Acad. Sci. USA* **74,** 5463–5467 (1977).
27. Choi, Y. *et al.* Single-molecule lysozyme dynamics monitored by an electronic circuit. *Science* **335,** 319–324 (2012).
28. Warshel, A. *et al.* Electrostatic basis for enzyme catalysis. *Chem. Rev.* **106,** 3210–3235 (2006).

29. Chen, Y. S., Hong, M. Y. & Huang, G. S. A protein transistor made of an antibody molecule and two gold nanoparticles. *Nature Nanotech.* **7,** 197–203 (2012).
30. Huang, G. S., Chen, Y. S. & Yeh, H. W. Measuring the flexibility of immunoglobulin by gold nanoparticles. *Nano Lett.* **6,** 2467–2471 (2006).
31. Blanco, L. *et al.* Highly efficient DNA synthesis by the phage phi 29 DNA polymerase. Symmetrical mode of DNA replication. *J. Biol. Chem.* **264,** 8935–8940 (1989).
32. Reimar, J. *et al.* Rolling-circle amplification of viral DNA genomes using phi29 polymerase. *Trends Microbiol.* **17,** 205–211 (2009).
33. McCarthy, D., Bemstein, H. & Bemstein, C. DNA elongation rates and growing point distributions of wild-type phage T4 and a DNA-delay amber mutant. *J. Mol. Biol.* **106,** 963–981 (1976).
34. Ella, B., Stanley, T. & Charles, C. R. The thioredoxin binding domain of bacteriophage T7 DNA polymerase confers processivity on *Escherichia coli* DNA polymerase I. *Proc. Natl Acad. Sci. USA* **94,** 479–484 (1997).
35. Camps, M. & Loeb, L. A. When pol I goes into high gear: processive DNA synthesis by pol I in the cell. *Cell Cycle* **3,** 116–118 (2004).
36. English, B. P. *et al.* Ever-fluctuating single enzyme molecules: Michaelis–Menten equation revisited. *Nature Chem. Biol.* **2,** 87–94 (2006).

Acknowledgements

This work was partially supported by the 'Aim for the Top University Plan' of the National Chiao Tung University and the Ministry of Education, Taiwan, ROC. This work was also partly supported by Nanotechnology National project 101-2120-M-009-008 of the National Science Counsel, Taiwan, and a National Health Research Institute grant (NHRI-EX102-10249EI). The authors acknowledge funding support from the Air Force Office of Scientific Research (AFOSR, FA2386-11-1-4094; special grant AOARD-13-4035).

Author contributions

Y.S.C. and G.S.H. are responsible for the concept and design of the study. G.S.H., C.H.L. and M.Y.H. prepared the manuscript. Y.S.C., C.H.L., H.A.P., J.C.C. and M.Y.H performed the experiments and data analysis.

Additional information

Supplementary information is available in the online version of the paper. Reprints and permissions information is available online at www.nature.com/reprints. Correspondence and requests for materials should be addressed to G.S.H.

Competing financial interests

The authors declare no competing financial interests.

ERRATUM

DNA sequencing using electrical conductance measurements of a DNA polymerase

Yu-Shiun Chen, Chia-Hui Lee, Meng-Yen Hung, Hsu-An Pan, Jin-Chern Chiou and G. Steven Huang

Nature Nanotechnology **8,** 452–458 (2013); published online 5 May 2013; corrected after print 11 July 2013.

In the version of this Article originally published, the addresses of all affiliations were incorrect; the correct addresses should have read "[1]Department of Biological Science and Technology, National Chiao Tung University, 1001 University Road, Hsinchu, Taiwan, ROC, [2]Biomedical Electronics Translational Research Center, National Chiao Tung University, 1001 University Road, Hsinchu, Taiwan, ROC, [3]Department of Materials Science and Engineering, National Chiao Tung University, 1001 University Road, Hsinchu, Taiwan, ROC, [4]Institute of Electrical and Control Engineering, National Chiao Tung University, 1001 University Road, Hsinchu, Taiwan, ROC." In the Acknowledgements, the first sentence should have read "This work was partially supported by the 'Aim for the Top University Plan' of the National Chiao Tung University and the Ministry of Education, Taiwan, ROC." These errors have been corrected in the HTML and PDF versions.

ADDENDUM

DNA sequencing using electrical conductance measurements of a DNA polymerase

Yu-Shiun Chen, Chia-Hui Lee, Meng-Yen Hung, Hsu-An Pan, Jin-Chern Chiou and G. Steven Huang

Nature Nanotechnology **8,** 452–458 (2013); published online 05 May 2013; corrected after print 11 July 2013 and 28 August 2013.

Editorial note: significant concerns have been raised about the validity of the data reported in this work. After an internal inquiry, we contacted the authors' institution, the National Chiao Tung University, and asked them to launch a formal investigation into the matter. This investigation is now underway.